Full wavefield migration based on eigen-decomposition propagation operators

Li, A.; Verschuur, D.J.; Abolhassani, S.

DOI
10.3997/2214-4609.2023101469

Publication date
2023

Document Version
Final published version

Citation (APA)
Li, A., Verschuur, D. J., & Abolhassani, S. (2023). *Full wavefield migration based on eigen-decomposition propagation operators*. Paper presented at 84th EAGE ANNUAL Conference and Exhibition 2023, Vienna, Austria. https://doi.org/10.3997/2214-4609.2023101469

Full wavefield migration based on eigen-decomposition propagation operators

A. Li[1,2], D.J. Verschuur[1], S. Abolhassani[1]

[1] Delft University Of Technology; [2] China University of Geosciences (Beijing)

Summary

Seismic imaging is crucial for subsurface exploration and monitoring, with a focus on deep and complex structures. Seismic wave migration solves the wave equation, and an accurate propagator is essential. Full Wavefield Modeling (FWMod) was developed based on recursive and iterative up/down wavefield propagation, modeling both primaries and multiples. Embedded within Full Wavefield Migration (FWM) it can be used to image data including multiples, resulting in better illumination in case primary illumination is not sufficient. FWM can be efficient and effective, but conventional one-way wave operators, such as Phase Shift Plus Interpolation Migration, have limitations in strongly inhomogeneous media. Local velocity-based one-way operator based on eigen decomposition was proposed and integrated within FWMod and FWM in this study, improving image amplitudes and fidelity and improving converage speed in the least-squares inversion process.

Full wavefield migration based on eigen-decomposition propagation operators

Introduction

Seismic imaging is a critical process for exploration and monitoring, particularly in deep and complex structures. The goal of seismic wave migration is to solve the wave equation, making an accurate propagator crucial for success. Conventional migration treats multiples as noise and removes them during migration, but properly handling multiples is crucial for accurate seismic imaging. Full Wavefield Modeling (FWMod), based on recursive and iterative up/down one-way wave-propagation, was developed to model both primaries and multiples (Berkhout 2014a; Davydenko and Verschuur, 2017). Full Wavefield Migration (FWM) algorithm is employed to image the data including multiples, resulting in better illumination (Berkhout 2014b). FWM has much potential for development due to its high computational efficiency and less wavefield storage compared to reverse time migration (Liu et al., 2015).

However, the conventional one-way wave operator used in FWM, such as Phase Shift or Phase Shift Plus Interpolation (PSPI) Migration, has limitations when dealing with strongly inhomogeneous media due to its global velocity approximation (Gazdag and Sguazzero, 1984). To address this, local velocity-based one-way operators have been proposed, which calculate a local homogeneous solution for the velocity at each grid node and can accommodate arbitrarily variant velocity media (Kosloff and Kessler, 1987; Grimbergen et al., 1998; Hammad and Verschuur, 2016; Li and Liu, 2021). In this study, we integrated the one-way wave operator based on eigen decomposition (ED) into the FWMod and FWM framework to make it better suited for heterogeneous media, resulting in improved imaging amplitude and accelerated converage speed.

Eigen decomposition operator for FWM

The Full Wavefield Modeling approach involves decomposing the wavefield into two components, namely a downgoing component represented by P^+ and an upgoing component represented by P^-. This representation is made regarding a preferred direction, which is typically the vertical direction. Additionally, the method categorizes the wavefield by its order of scattering j. The source extrapolation equation can be expressed for one frequency component, as described by Berkhout (2014a):

$$P_j^{\pm}(z_m^-, z_0) = \mathbf{W}^{\pm}(z_m^{\mp}, z_0) S_j^{\pm}(z, \omega) + \sum_{n=0}^{m-1} \mathbf{W}^{\pm}(z_m^{\mp}, z_n^{\pm}) \delta S_j^{\pm}(z_m^{\pm}, z_0) \,, \tag{1}$$

where the equation involves a physically induced source at depth level z, denoted by S, which can be either blended or unblended. The vectors represent monochromatic wavefields for one original source experiment j In addition, there is a secondary source, δS, triggered by the medium in response to an incident wavefield. It also mentions the matrices $W^{\pm}(z_m^{\mp}, z_0)$ represent the scattering-free downward and upward propagation operators, respectively, between depth levels z_0 and z_m (n > m). The secondary source is connected to the medium parameters through the following relationship

$$\delta S_j^{\pm}(z_n^{\mp}, z_0) = \mathbf{R}(z_n^{\pm}, z_n^{\pm}) P_j^{\mp}(z_n^{\pm}; z_0) + \delta \mathbf{T}^{\pm}(z_n^{\pm}, z_n^{\mp}) P_j^{\pm}(z_n^{\mp}; z) \,, \tag{2}$$

where $\boldsymbol{R}$ and $\boldsymbol{T}$ represent the vertical components of reflection and transmission operators.

The common approach for computing wavefields in neighboring layers involves using a one-way wave migration operator is

$$\mathbf{W}^{\pm} = e^{\mp i \Lambda \Delta z} \,, \tag{3}$$

where Δz is the depth step, and $\boldsymbol{\Lambda}$ represents the square root operator.With the relationship of the Helmholtz operator $\mathbf{\Lambda}^2$, as

$$\mathbf{\Lambda}^2 = \frac{\omega^2}{v(x)^2} + \frac{\partial^2}{\partial x^2} \,, \tag{4}$$

in which a second-order discretization of $\partial^2/\partial x^2$ is included, can be written for a depth level as

$$\mathbf{\Lambda}^2 = \begin{bmatrix} \frac{\omega^2}{v^2(x_1)} & 0 & \cdots & 0 \\ 0 & \frac{\omega^2}{v^2(x_2)} & \cdots & 0 \\ \vdots & \vdots & \ddots & \vdots \\ 0 & 0 & \cdots & \frac{\omega^2}{v^2(x_n)} \end{bmatrix} + \begin{bmatrix} \frac{2}{(\Delta x)^2} & \frac{1}{(\Delta x)^2} & 0 & 0 \\ \frac{1}{(\Delta x)^2} & \frac{2}{(\Delta x)^2} & \ddots & 0 \\ 0 & \ddots & \ddots & \frac{1}{(\Delta x)^2} \\ 0 & 0 & \frac{1}{(\Delta x)^2} & \frac{2}{(\Delta x)^2} \end{bmatrix}. \tag{5}$$

This matrix can effectively manage variations in lateral velocity in horizon coordination, thanks to the diagonal elements contained within the matrix. These diagonal elements correspond to all velocity points located at a specific depth. Note that the matrix is constructed using a second-order finite-difference discretization technique, but to improve the accuracy for FWMod and FWM, it is recommended to be substituted with a higher-order discretization method.

With matrix transformation theory, the self-adjoint matrix $\mathbf{\Lambda}^2$ can be factorized into the product of its eigenvalues and eigenvectors as

$$\mathbf{\Lambda}^2 = \mathbf{VMV}^{\mathrm{T}}, \tag{6}$$

where the matrix $\mathbf{M}$ and $\mathbf{V}$, respectively, denote the eigenvalues and eigenvectors of $\mathbf{\Lambda}^2$, and the superscript T represents the matrix transpose. Using the matrix eigen decomposition theory framework, the eigenvalues of matrix functions are dependent on the eigenvalues of the original matrix, while their eigenvectors remain constant. Consequently, the eigenvalues and eigenvectors of the sub-functions can be represented as such.

$$\mathbf{\Lambda} = \mathbf{V}\sqrt{\mathbf{M}}\mathbf{V}^{\mathrm{T}}, \tag{7}$$

$$\mathbf{W}^{\pm} = \mathbf{V}e^{\mp i\sqrt{\mathbf{M}}\Delta z}\mathbf{V}^{\mathrm{T}}. \tag{8}$$

In depth-domain wavefield extrapolation, it is crucial to address the issue of evanescent waves. If the eigenvalue is real-valued, significant waves propagate during extrapolation. However, the presence of evanescent waves can lead to instability as they grow exponentially with depth. The growth of evanescent waves is attributed to complex-valued eigenvalues. To mitigate this issue, by keeping the real-valued eigenvalues and disregarding the complex-valued ones, our approach is straightforward to eliminate the evanescent waves.

Numerical example

The size of the velocity model is 1000 × 2000 m with a grid of 20 × 20 m, which has a strong lateral velocity contrast and steep dipping angles, as shown in Figure 1a. We use this model to verify the imaging performance of the proposed FWM algorithm. Figure 1b is the true reflectivity model. The shot gathers were generated by the full wavefield modeling with 5th-order multiples. The shot distance and receiver distance are 100 m and 20 m respectively.

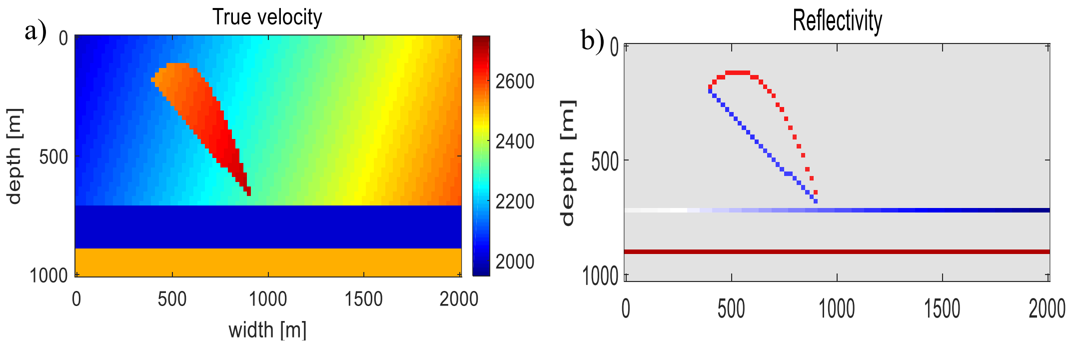

Figure 1 *Velocity model. (a) The true velocity model; (b) the true reflectivity model.*

The four sub-figures in Figure 2 provide a comprehensive representation of the real and imaginary components of the complex propagation operator at a depth of 300 m with a frequency of 10 Hz. Specifically, Figures 2a and 2b display the real and imaginary parts, respectively, of the conventional PSPI operator, while Figures 2c and 2d illustrate the real and imaginary parts of the ED operator, respectively. From this picture, we can see that the ED operator is more sensitive to lateral velocity changes at a depth level.

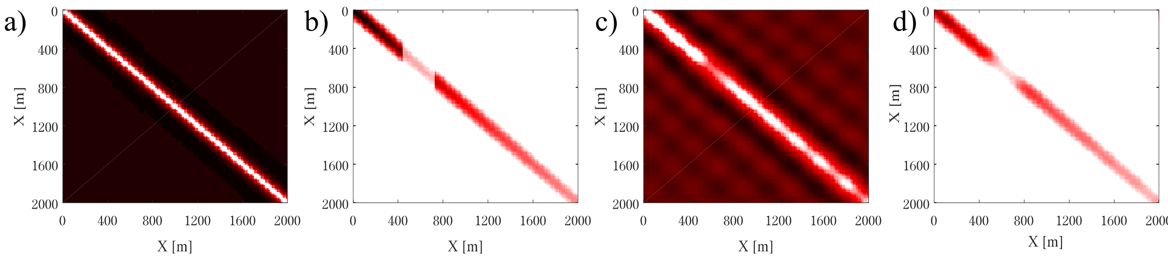

***Figure 2** The real and imaginary of the complex propagation operator at 400m depth with 10 Hz. (a) the real part of the conventional PSPI operator; (b) the imaginary part of the conventional PSPI operator; (c) the real part of the ED operator; (d) the imaginary part of the ED operator.*

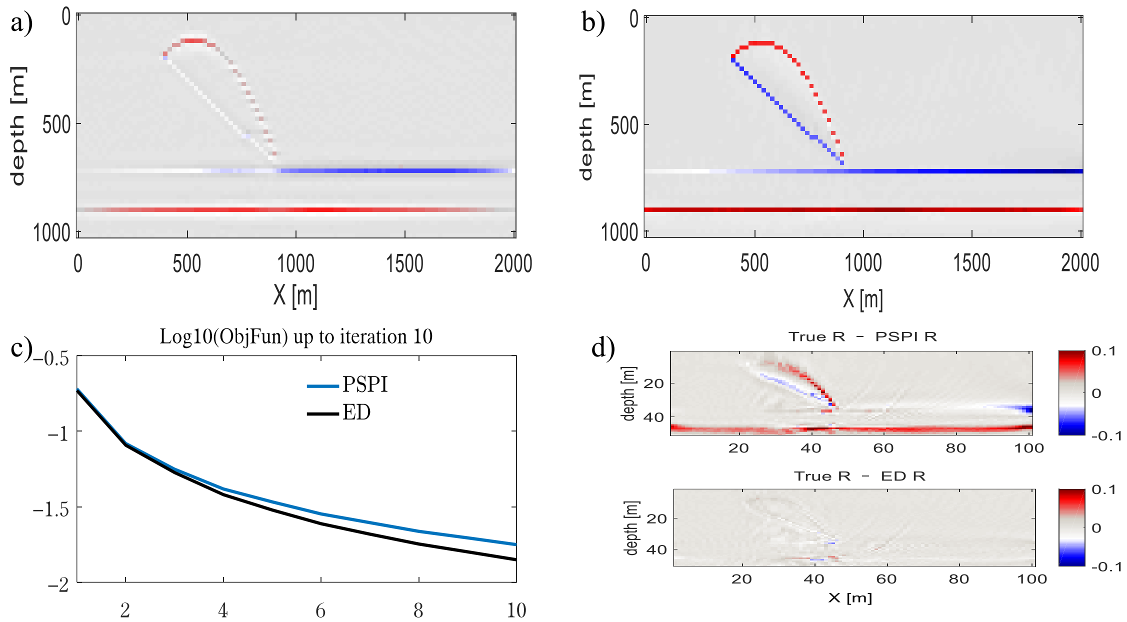

***Figure 3** The imaging section after (a) 1 iteration and (b) 10 iterations of the ED operator; (c) objective function compared with the conventional PSPI operator in FWM, and (d) the difference between true reflectivity and estimated reflectivity for the two operators.*

The imaging outcomes for 1 and 10 iterations are presented in Figures 3a and 3b, respectively. Figure 3c shows the objective function converges curve compared with the conventional PSPI operator in FWM, which reveal the fast convergence speed of our method. Figure 3d shows the difference between true reflectivity and estimated reflectivity of using the conventional PSPI operator and the proposed ED operator, as a certification that our method can better recover reflectivity. Furthermore, Figure 4 displays the imaging amplitude and reflectivity at different positions. Specifically, Figure 4a illustrates the imaging amplitude at a specific location on the x-axis (x=860 m), while Figure 4b depicts the reflectivity at a particular depth of 740 m.

Comparison with the true model and imaging section reveals that the proposed algorithm can effectively handle strong velocity contrasts, accurately depict the structure, and achieve true-amplitude reflectivity recovery as a true amplitude method. Notably, the amplitude and reflectivity curves illustrate that the algorithm considers transmission compensation and multiple imaging, thereby enabling us to obtain a true amplitude migration result. Compared with the PSPI operator, the ED operator gets more accurate amplitudes calculation.

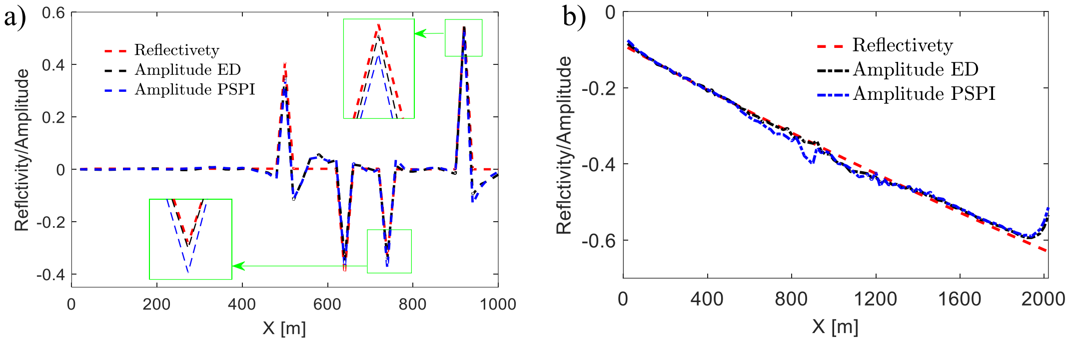

Figure 4 *Imaging amplitude and reflectivity. (a) X=860 m (b) Depth=740 m.*

Conclusions

This study proposed a novel approach that incorporated an eigendecomposition-based one-way wave operator into the full wavefield migration framework. Through the computation of eigenvalues and eigenvectors of the Helmholtz operator, an operator that characterizes the behavior of the wavefield during subsurface propagation was constructed. The true-amplitude imaging capabilities of this approach were verified by examining wavefield propagation in the model with pronounced lateral velocity heterogeneity.

Acknowledgments

The authors thank the China Scholarship Council and Delphi consortium for their financial support.

References

Berkhout, A.J. [2014a] Review paper: An outlook on the future of seismic imaging, Part I: Forward and reverse modelling. *Geophysical Prospecting*, **62**, 911–930.

Berkhout, A.J. [2014b] Review Paper: An outlook on the future of seismic imaging, Part II: Full-Wavefield Migration. *Geophysical Prospecting*, **62**(5), 931–949.

Davydenko, M. and Verschuur, D.J. [2017] Full-Wavefield Migration: using surface and internal multiples in imaging. *Geophysical Prospecting*, **65**, 7-21.

Gazdag, J. and Sguazzero P. [1984] Migration of seismic data by phase shift plus interpolation. *Geophysics*, **49**, 124–131.

Grimbergen, J.L.T., Dessing, F.J. and Wapenaar, K. [1998] Modal expansion of one-way operators in laterally varying media. *Geophysics*, **63**(3), 995–1005.

Hammad, H.I. and Verschuur D.J. [2016] Joint migration inversion for laterally varying media. In: *78th EAGE Conference and Exhibition 2016*.

Kosloff, D and Kessler, D. [1987] Accurate depth migration by a generalized phase-shift method. *Geophysics*, **52**(8), 1074-1084.

Li, A.Y. and Liu, X.W. [2021] An optimised one-way wave migration method for complex media with arbitrarily varying velocity based on eigen-decomposition. *Journal of Geophysics and Engineering*, **18** (5), 776–787.

Liu, Y. K., Hu, H., Xie, X.B., Zheng, Y.C. and Li, P. [2015] Reverse time migration of internal multiples for subsalt imaging. *Geophysics*, **80** (5), S175-S185.